Polyadic devil's lenses

Arnau Calatayud,[1] Juan A. Monsoriu,[1,*] Omel Mendoza-Yero,[2,3] and Walter D. Furlan[4]

[1]*Centro de Tecnologías Físicas, Universidad Politécnica de Valencia, E-46022 Valencia, Spain*
[2]*Departament de Física, GROC-UJI, Universitat Jaume I, 12080 Castelló, Spain*
[3]*Institut de Noves Tecnologies de la Imatge, Universitat Jaume I, 12080 Castelló, Spain*
[4]*Departamento de Óptica, Universidad de Valencia, E-46100 Burjassot (Valencia), Spain*
**Corresponding author: jmonsori@fis.upv.es*

Received August 31, 2009; accepted September 28, 2009;
posted October 6, 2009 (Doc. ID 116537); published November 9, 2009

Devil's lenses (DLs) were recently proposed as a new kind of kinoform lens in which the phase structure is characterized by the "devil's staircase" function. DLs are considered fractal lenses because they are constructed following the geometry of the triadic Cantor set and because they provide self-similar foci along the optical axis. Here, DLs are generalized allowing the inclusion of polyadic Cantor distributions in their design. The lacunarity of the selected polyadic fractal distribution is an additional design parameter. The results are coined polyadic DLs. Construction requirements and interrelations among the different parameters of these new fractal lenses are also presented. It is shown that the lacunarity parameter affects drastically the irradiance profile along the optical axis, appodizing higher-order foci, and these features are proved to improve the behavior of conventional DLs under polychromatic illumination. © 2009 Optical Society of America

OCIS codes: 050.1940, 050.1965.

1. INTRODUCTION

Fractals are geometric objects having certain special properties of homogeneity and self-similarity that may describe naturally occurring fragmented and irregular structures [1]. Fractal geometry is exceptionally fruitful. It has been identified in many diverse scientific areas such as biology, medicine, electric circuits, geomorphology, fracture theory, and even stock markets. From a mathematical point of view, fractals are obtained by performing a basic operation, called *generator*, on a given geometrical object, called *initiator*. Thus, the generator is a collection of scaled N-copies of the initiator. By applying successively the same process over smaller and smaller scales on the resultant objects, an object composed of subunits of itself is created. Mathematically, the above property should hold on all (infinite) scales. However, in the real world, there are necessarily lower and upper bounds between which such self-similar behavior applies.

The simplest fractal is the triadic Cantor set [1]. It is a 1-D object where the scale of the copies in the generator is 1/3. The generalization of this elementary structure is the polyadic Cantor set with variable lacunarity. These structures have recently found applications in the design of fractal engineering devices, such as dielectric multilayers [2], Cantor ring difractals [3], or semiconductor multilayers [4]. In the above applications the lacunarity was introduced as a new free design.

Fractal zone plates (FZPs) where introduced in 2003 as curious diffractive elements with many potential applications. The main characteristic of a FZP is its fractal structure along the squared radial coordinate. It has been shown that FZPs have multiple foci, replicating the lens fractality along the optical axis [5]. The number of foci and their relative amplitude can be modified with the lacunarity in the design stage [6]. Since their introduction, FZPs have received the attention of several research groups working on diffractive optics [7,8]. It has been shown that in certain applications FZPs can improve the performance of classical Fresnel zone plates. For instance, we can profit from FZPs in image-forming systems [9], versatile optical tweezers [10], design of novel optical filters [11], and optical cryptography [12].

Recently introduced, devil's lenses (DLs) are new members of the FZP family [13]. These are kinoform lenses in which the phase distribution is characterized by the "devil's staircase" generated with the triadic Cantor set. It has been shown that DLs drive most of the incoming light into one single focus, improving in this way the efficiency of FZPs. An experimental characterization of a multilevel phase version of a DL has also been reported [14].

In this paper, we propose a generalization of the concept of DLs by the inclusion of polyadic Cantor distributions in their design. The result is thus a polyadic DL (PDL). The lacunarity of the selected polyadic fractal distribution is an additional design parameter. Other practical considerations related to the design of these lenses are presented. The axial irradiance originated by PDLs based on regular polyadic fractals are numerically evaluated and compared with the response of equivalent kinoform lenses. The effect of lacunarity on the axial irradiance of a PDL is investigated. We show how to use this parameter to improve the response of conventional DLs under polychromatic illumination.

2. BASIC THEORY

Let us consider the irradiance at a given point on the optical axis due to a rotationally invariant pupil with a transmittance $p(r)$ illuminated by a monochromatic plane

wave. Within the Fresnel approximation, the above irradiance is given as a function of the axial distance from the pupil plane z as

$$I(z) = \left(\frac{2\pi}{\lambda z}\right)^2 \left| \int_0^a p(r_o) \exp\left(-i\frac{\pi}{\lambda z} r_o^2\right) r_o dr_o \right|^2. \quad (1)$$

In Eq. (1), a is the maximum extent of the pupil function $p(r)$, and λ is the wavelength of light. For our purposes it is convenient to express the transmittance of the pupil as function of a new variable, that is

$$\varsigma = \left(\frac{r_o}{a}\right)^2, \quad (2)$$

in such a way that $q(\varsigma)=p(r_0)$. By using the reduced axial coordinate $u=a^2/2\lambda z$, the irradiance along the optical axis can now be given in terms of the Fourier transform of $q(\varsigma)$ by the expression

$$I(u) = 4\pi^2 u^2 \left| \int_0^1 q(\varsigma) \exp(-i2\pi u\varsigma) d\varsigma \right|^2. \quad (3)$$

For DLs, $q(\varsigma)$ is a self-similar function constructed from the fractal Cantor set whose generation procedure is shown in Fig. 1. In the first stage ($S=1$), the initial segment is divided into an odd number of segments $2N-1$, and then segments in the even positions are removed. For the remaining N segments at the first stage, the above "slicing and removing" process is repeated in the second stage, and so on. In the original proposal of a DL [11] the triadic Cantor set was studied ($2N-1=3$). Here, we propose PDLs that are more general structures, constructed from different levels of a polyadic Cantor set. To consider an example, Fig. 1 shows a heptadic Cantor set with $N=4$ remaining segments at $S=1$.

In general, at stage S there are N^S segments of length N^S with N^S-1 disjoint gaps intervals $[p_{S,l}, q_{S,l}]$, with $l=1,\ldots,N^S-1$. Based on this fractal structure, the Cantor function $F_S(x)$, also known as devil's staircase [15], can be defined within the interval [0, 1] as

$$F_S(x) = \begin{cases} \dfrac{l}{N^S}, & \text{if } p_{S,l} \le x \le q_{S,l} \\ \dfrac{1}{N^S}\dfrac{x-q_{S,l}}{p_{S,l+1}-q_{S,l}} + \dfrac{l}{N^S}, & \text{if } q_{S,l} \le x \le p_{S,l+1} \end{cases}, \quad (4)$$

where $F_S(0)=0$ and $F_S(1)=1$. Therefore, the devil's staircase $F_S(x)$ takes within the gaps intervals of the Cantor set the constant values l/N^S with $l=1,\ldots,N^S-1$; meanwhile, between these intervals, the continuous function $F_S(x)$ is linearly increasing (see Fig. 2). The corresponding

Fig. 1. Polyadic Cantor set ($N=4$) for the levels $S=0$, 1, 2. The structure for $S=0$ if the initiator and the one corresponding to $S=1$ is the generator.

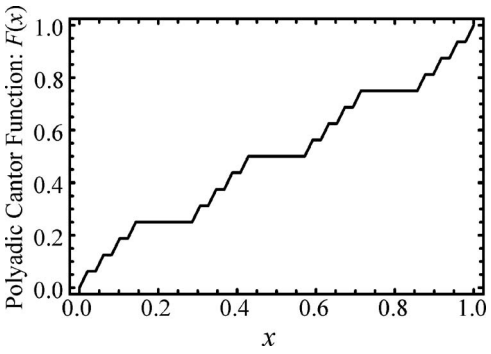

Fig. 2. Polyadic Cantor function or Polyadic devil's staircase for $N=4$, $S=2$.

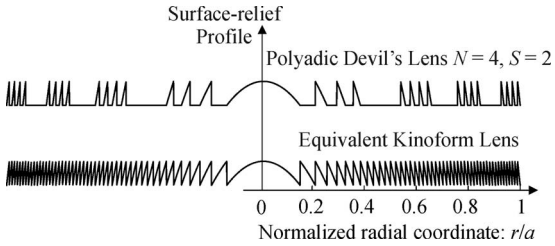

Fig. 3. Convergent PDL for N=4, S=2 and the equivalent kinoform Fresnel lens.

PDL can be defined from $F_S(x)$ as a circularly symmetric diffractive optical element with a phase profile that follows the polyadic Cantor function at a given stage S. At the gap regions defined by the Cantor set the phase shift is $-l2\pi$, with $l=1,\ldots,N^S-1$. Thus, the transmittance of the PDL is defined by

$$q(\varsigma) = q_{DL}(\varsigma, S) = \exp[-iN^s 2\pi F_S(\varsigma)]. \quad (5)$$

The surface-relief profile $h(r)$ corresponding to the above phase function can be obtained from the relation [16]

$$h_{DL}(r) = \mathrm{mod}_{2\pi}\left\{-N^s 2\pi F_S\left(\frac{r^2}{a^2}\right)\right\}\frac{\lambda}{2\pi(n-1)}, \quad (6)$$

where $\mathrm{mod}_{2\pi}[\varphi(r)]$ is the phase function $\varphi(r)$ modulo 2π, n is the refractive index of the optical material used to construct the lens, and λ is the wavelength of the light.

Figure 3 shows the profile of a PDL generated from a heptadic Cantor set ($N=4$), up to $S=2$. Note that because of the change of variables in Eq. (2), the phase profile variation in each zone of the lens is quadratic.

3. FOCUSING PROPERTIES OF PDLS

The axial irradiance of the PDL computed for different stages of growth S and for $N=4$ is shown in Figs. 4 and 5. For comparison, the irradiance of the associated Fresnel kinoform lens is shown in the same figures. The irradiance normalization criterion is the same in both figures. Note that the scale for the axial coordinate in each step is a demagnified version of the one in the previous step (S) by a factor $2N-1=7$. It can be seen that for the PDL the axial positions of the central lobes coincide with those of the associated Fresnel lens. For both types of lenses, we

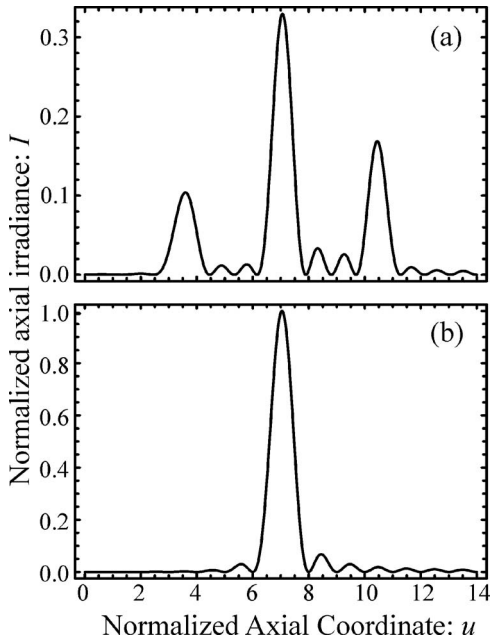

Fig. 4. Normalized irradiance vs. the axial coordinate u obtained (a) for a regular PDL ($N=4$, $S=1$) and (b) for its associated Fresnel kinoform lens.

find a main focus at the normalized distance $u_0=(2N-1)^S$ corresponding to a focal length

$$f(N,S)=\frac{a^2}{2\lambda(2N-1)^S}. \tag{7}$$

Note that a PDL exhibits subsidiary foci with a characteristic fractal profile; i.e, the axial irradiance produced by a lens constructed with $S=2$ is a modulated version of that corresponding to $S=1$. In fact, any wide focus at stage $S=1$ is transformed into three narrower foci at stage $S=2$ that are scale-invariant over dilations of factor $2N-1=7$. This *axial scale property* holds for any N and has been found previously for the amplitude FZP [5]. It means that, for a PDL, the axial irradiance also reproduces the self-similarity of the lens itself. To investigate this property quantitatively, we use the following correlation coefficient between the axial irradiance Eq. (3) and the same function but with a variable scale factor γ [17]:

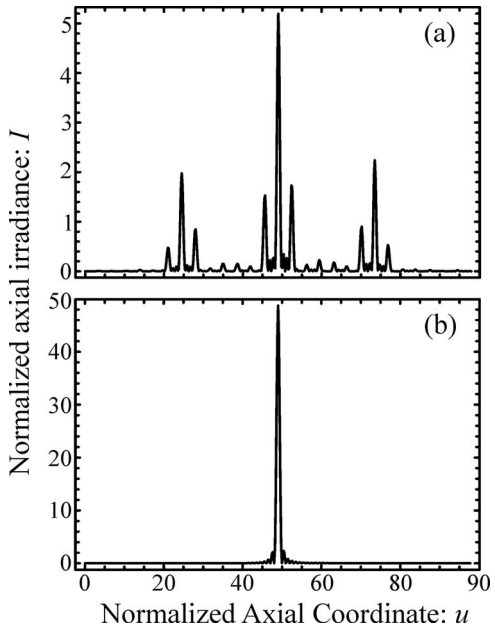

Fig. 5. Normalized irradiance vs. the axial coordinate u obtained (a) for a regular PDL ($N=4$, $S=2$) and (b) for its associated Fresnel kinoform lens.

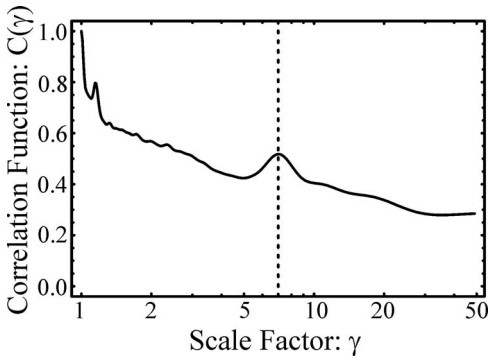

Fig. 6. Correlation function $C(\gamma)$ for the axial irradiance shown in Fig. 5(a).

$$C(\gamma)=\frac{\int_{-\infty}^{\infty} I(u)\cdot I\left(u_0+\frac{u-u_0}{\gamma}\right)\mathrm{d}u}{\sqrt{\int_{-\infty}^{\infty} I^2(u)du\int_{-\infty}^{\infty} I^2\left(u_0+\frac{u-u_0}{\gamma}\right)\mathrm{d}u}}. \tag{8}$$

This function was computed for the irradiance of a PDL with $N=4$ and $S=2$. The result is shown in Fig. 6. It can be seen that when the axial irradiance satisfies the strict axial self-similar property $I(u)=I(u_0+(u-u_0)/\gamma)$, the correlation coefficient (or simply, the self-similarity) is $C(\gamma)=1$. Lower degrees of self-similarity give values of $C(\gamma)$ lower than unity. Thus, some local maxima of the curve are expected to appear at $\gamma=(2N-1)^i$, $i=1,2,\ldots S$. A local maxima at $\gamma=7$ is evident in this figure. The local maxima corresponding to $\gamma=49$ (not shown in Fig. 6) is much lower than the previous one.

4. PDLS WITH VARIABLE LACUNARITY

In the previous section, PDLs were constructed from regular fractal structures in the sense that clear and dark regions have the same size; see Fig. 1. When the lacunarity parameter is taken into account, a more general PDL can be defined. The construction of a typical *polyadic* Cantor fractal set with a specific lacunarity is shown in Fig. 7. First step in the construction procedure consists of defining the initiator at stage $S=0$. Next, at stage $S=1$, the generator is constructed by N non-overlapping copies of

Fig. 7. Polyadic Cantor set with variable lacunarity ($N=4$).

the initiator, each one with a scale $\gamma<1$. To characterize the resulting Cantor set, one of the most frequently used descriptors is the fractal dimension, defined as

$$D = -\frac{\ln(N)}{\ln(\gamma)}. \tag{9}$$

However, fractal dimension does not uniquely define the fractal. For the general case, it is necessary to introduce another parameter to specify the distribution of the N copies into the unit length segment. The additional parameter specifies the lacunarity of the resulting structure and it is essential to carry out a complete characterization of the fractal. Note that structures with different lacunarity can have the same fractal dimension. Following the convention adopted in some previous papers dealing with Cantor fractals [2,4,6] we use the width of the outermost gap in the first stage, ε, to define the lacunarity. Then, for even N, half of the copies are placed to the left of the interval and the remaining half to its right. All copies are separated by a fixed distance ε. For odd N, one copy lies exactly centered in the interval, with $\lfloor N/2 \rfloor$ copies placed to the left of the interval and the remaining $\lfloor N/2 \rfloor$ to its right. Here, $\lfloor N/2 \rfloor$ is the greatest integer less than or equal to $\lfloor N/2 \rfloor$. In Fig. 7 the parameters $N=4$, $\gamma=1/7$, and $\varepsilon=0.075$ have been selected. At the following stages of construction of the set ($S=2,3,\ldots$), the generation process is repeated over and over again for each segment in the previous stage.

Therefore, symmetric polyadic Cantor fractals are characterized by three parameters: the number of self-similar copies N, the scaling factor γ, and the lacunarity ε. The last two parameters must satisfy certain constraints to avoid overlapping between the copies. On the one hand, the maximum value of the scaling factor depends on the value of N, such that $0<\gamma_{\max}<1/N$. In addition, for each N and γ, the parameter ε can take values only within the range $[0,\varepsilon_{\max}]$. When $\varepsilon=0$, the highest lacunar fractal is obtained. In this case, for even N, the central gap has a width of $1-N\gamma$, and for odd N, both large gaps surrounding the central segment have a width of $(1-N\gamma)/2$. On the other hand, it is easy to show that the values for $\varepsilon_{\max}$ are the following:

$$\varepsilon_{\max} = \begin{cases} \dfrac{1-N\gamma}{N-2}, & \text{even } N \\ \dfrac{1-N\gamma}{N-3}, & \text{odd } N \end{cases}. \tag{10}$$

Thus, for $\varepsilon_{\max}$ the inner segments (two for even N, or three for odd N) join together in the center. Between $\varepsilon=0$ and $\varepsilon=\varepsilon_{max}$ there is a particular value of ε that gives the lowest lacunar (or *regular*) fractal. This value of ε, obtained after imposing bars and gaps to have the same size at the initiatior stage, is given by

$$\varepsilon_R = \frac{1-N\gamma}{N-1}. \tag{11}$$

Note that the lacunarity parameter ε defines gaps intervals $[p_{S,l},q_{S,l}]$ in Eq. (4), modifying the transmittance of the PDL. To show that self-similar behavior of the axial irradiance for PDL is retained, even when the lacunarity is varied, twist plots are used. In these plots, the axial irradiance given by Eq. (3) is represented as a function of the normalized axial distance and the lacunarity parameter ε. Figure 8 shows twist plots for PDLs with $N=4$ at stage of growth $S=1$ (a) and S=2 (b). Note that, a linear grayscale was used for the normalized axial irradiance. In this case the lacunarity parameter ε is limited by $\varepsilon_{min}=0$ and $\varepsilon_{max}=3/14$. It is obvious that the optical irradiance originated by the PDLs is highly influenced by the lacunarity. The axial irradiance nulls in the above figures can be understood as multiple cross-interferences among different phase rings of the PDL. The most noticeable feature in Fig. 8 is the self-similarity that can be observed between the plots corresponding to $S=1$ and $S=2$. In fact, the rescaled data at stage $S=1$ form an envelope for the data at $S=2$, and both structures are self-similar for any value of ε. This result shows that the axial irradiance provided by a PDL has self-similar properties like those reported for a lacunar FZP [6]. However, as the lacunar FZP produces multiple fractal foci along the optical axis, the irradiance produced by a PDL vanishes outside of the axial intervals shown in Fig. 8. Hence, the diffraction efficiency of PDLs is significantly improved with respect to FZPs.

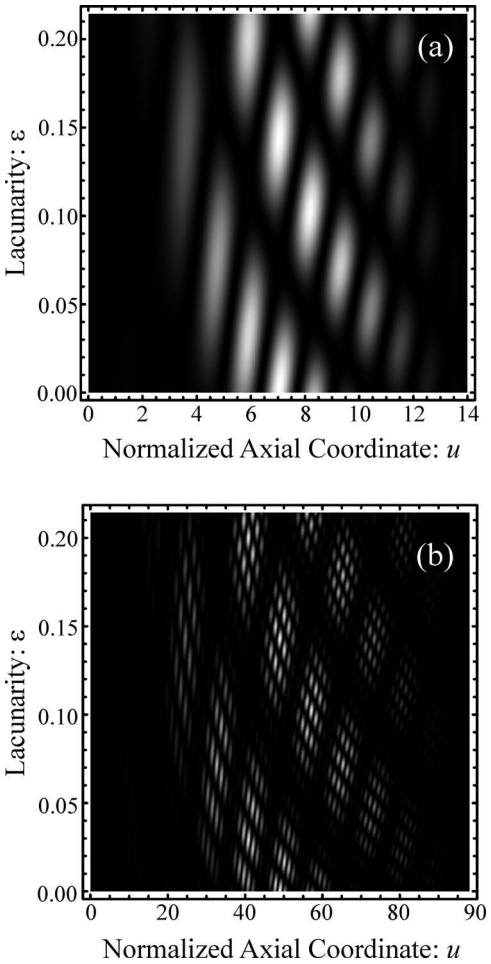

Fig. 8. Grayscale representation of the axial response plotted as a function of the normalized axial distance and the lacunarity of a PDL ($N=4$, $\gamma=1/7$) with variable lacunarity for: (a) $S=1$, (b) $S=2$.

5. PDLS WITH VARIABLE LACUNARITY UNDER POLYCHROMATIC ILLUMINATION

When using broadband illumination the monochromatic irradiances provided by the diffractive lenses regarded so far are affected by chromatic dispersion. As proposed in [13], for a given DL the subsidiary foci can be considered an extended depth of focus for each wavelength. Their overlapping results in a diffractive optical element (DOE) that is less sensitive to chromatic aberration than the conventional Fresnel kinoform lens. This behavior can be further improved for a PDL by selecting an adequate value of the lacunarity.

Following the conventional approach, the behavior of a PDL under broadband illumination can be evaluated in terms of the tristimuli values [18] computed along the optical axis:

$$X = \int_{\lambda_2}^{\lambda_1} I(r=0,z;\lambda)S(\lambda)\bar{x}\mathrm{d}\lambda; \quad Y = \int_{\lambda_2}^{\lambda_1} I(r=0,z;\lambda)S(\lambda)\bar{y}\mathrm{d}\lambda;$$

$$Z = \int_{\lambda_2}^{\lambda_1} I(r=0,z;\lambda)S(\lambda)\bar{z}\mathrm{d}\lambda; \tag{12}$$

where $S(\lambda)$ is the spectral distribution of the source, $(\bar{x},\bar{y},\bar{z})$ are the three sensitivity chromatic functions of the detector, and (λ_1,λ_2) represent the considered wavelength interval. In particular, in the assessment of visual systems $(\bar{x},\bar{y},\bar{z})$ are usually the sensitivity functions of the human eye (CIE 1931), and the axial response is normally expressed in terms of the axial illuminance Y and the axial chromaticity coordinates x, y:

$$\mathrm{x} = \frac{X}{X+Y+Z}, \quad \mathrm{y} = \frac{Y}{X+Y+Z}. \tag{13}$$

To show the improved behavior of a PDL as compared with a conventional DL we have computed Eqs. (12) and (13) for the DL reported in [13] and for a PDL with structural parameters $S=1$, $N=4$, $\gamma=1/7$, and $\varepsilon=0.1215$. We considered 41 monochromatic irradiances numerically evaluated for equally spaced wavelengths ranging from 380 nm to 780 nm. The standard illuminant C was used as spectral distribution of the source. The design wavelength for both DOEs was $\lambda=550$ nm. The result is shown in Fig. 9. Clearly, the axial illuminance for the PDL is more uniform and has an increased depth of focus compared with the conventional DL [Fig. 9(a)]. The degree of achromatization is evident in the display of the chromaticity [Fig. 9(b)]. In this figure we have computed the chromaticity curve for the axial points around the main focus: $0.9<z/f<1.1$. The triangles and squares represent $z/f=0.9$ and $z/f=1.1$, respectively, while the circles represent $z=f$ for the design wavelength. It can be observed that the PDL exhibits a slower chromaticity variation than the DL, and also that almost the whole curve for this lens is closer to the point representing the white illuminant.

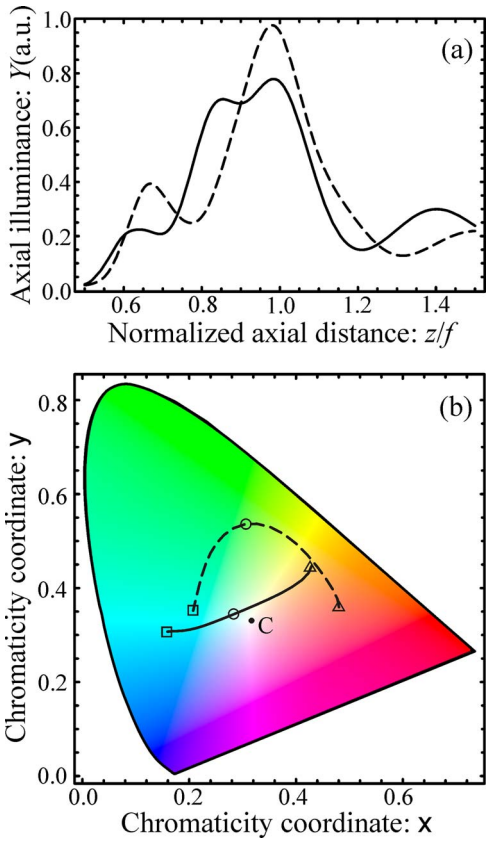

Fig. 9. (Color online) (a) Polychromatic axial illuminance computed for the conventional DL reported in [12] (dashed curve) and a PDL with structural parameters $S=1$, $N=4$, $\gamma=1/7$, $\varepsilon=0.1215$. The chromaticity of both curves is shown in (b).

6. CONCLUSIONS

Devil's lenses based on the polyadic Cantor set have been proposed. These lenses can be considered a more general family of fractal diffractive lenses. Several construction restrictions and interrelations among the different design parameters have been investigated. The focusing properties of PDL were analyzed and compared with those corresponding to a conventional Fresnel kinoform lens. It was shown that the lacunarity parameter has dramatic effects on the axial irradiance. This new design parameter allows us to improve the performance of fractal lenses, especially under white light illumination

The present study brings new insight into the powerful potential applications of DLs. These applications cover different scientific and technological areas that use diffractive optics, ranging from soft x-ray microscopy to THz imaging. A detailed study of the transverse irradiance distributions produced by PDLs as well as some aspects such as the influence of optical aberrations, the use of rotationally nonsymmetric phase zone plates, and the properties of vortex DLs, are currently underway.

ACKNOWLEDGMENTS

We acknowledge the financial support from grants DPI2006-8309 and DPI2008-02953 of Ministerio de Ciencia y Tecnología, Spain. We also acknowledge the support from Generalitat Valenciana through the project

PROMETEO2009-077 and from Universidad Politécnica de Valencia (PAID-06-08), Spain. Omel Mendoza-Yero is very grateful to the Spanish Ministry of Education and Science under Consolider Program Science and Applications of Ultrafast Ultraintense Lasers CSD2007-00013 for covering partial costs of the research.

REFERENCES

1. B. B. Mandelbrot, *The Fractal Geometry of Nature* (Freeman, 1982).
2. A. D. Jaggard and D. L. Jaggard, "Scattering from fractal superlattices with variable lacunarity," J. Opt. Soc. Am. A **15**(6), 1626–1635 (1998).
3. A. D. Jaggard and D. L. Jaggard, "Cantor ring difractals," Opt. Commun. **158**, 141–148 (1998).
4. F. R. Villatoro and J. A. Monsoriu, "Tunneling in quantum superlattices with variable lacunarity," Phys. Lett. A **372**, 3801–3807 (2008).
5. G. Saavedra, W. D. Furlan, and J. A. Monsoriu, "Fractal zone plates," Opt. Lett. **28**(12), 971–973 (2003).
6. J. A. Monsoriu, G. Saavedra, and W. D. Furlan, "Fractal zone plates with variable lacunarity," Opt. Express **12**, 4227–4234 (2004).
7. J. A. Davis, L. Ramirez, J. A. Rodrigo, T. Alieva, and M. L. Calvo, "Focusing properties of fractal zone plates: experimental implementation with a liquid-crystal display," Opt. Lett. **29**, 1321–1323 (2004).
8. H.-T. Dai, X. Wang, and K.-S. Xu, "Focusing properties of fractal zone plates with variable lacunarity: experimental studies based on liquid crystal on silicon," Chin. Phys. Lett. **22**, 2851–2854 (2005).
9. W. D. Furlan, G. Saavedra, and J. A. Monsoriu, "White-light imaging with fractal zone plates," Opt. Lett. **32**, 2109–2111 (2007).
10. S. H. Tao, X.-C. Yuan, J. Lin, and R. Burge, "Sequence of focused optical vortices generated by a spiral fractal zone plates," Appl. Phys. Lett. **89**, 031105 (2006).
11. O. Mendoza-Yero, G. Mínguez-Vega, M. Fernández-Alonso, J. Lancis, E. Tajahuerce, V. Climent, and J. A. Monsoriu, "Optical filters with fractal transmission spectra based on diffractive optics," Opt. Lett. **34**, 560–562 (2009).
12. M. Tebaldi, W. D. Furlan, R. Torroba, and N. Bolognini, "Optical-data storage-readout technique based on fractal encrypting masks," Opt. Lett. **34**, 316–318 (2009).
13. J. A. Monsoriu, W. D. Furlan, G. Saavedra, and F. Giménez, "Devil's lenses," Opt. Express **15**, 13858–13864 (2007).
14. D. Wu, L.-G. Niu, Q.-D. Chen, R. Wan, and H.-B. Sun, "High efficiency multilevel phase-type fractal zone plates," Opt. Lett. **33**, 2913–2915 (2008).
15. D. R. Chalice, "A characterization of the Cantor function," Am. Math. Monthly **98**, 255–258 (1991).
16. Y. Han, L. N. Hazra, and C. A. Delisle, "Exact surface-relief profile of a kinoform lens from its phase function," J. Opt. Soc. Am. A **12**, 524–529 (1995).
17. Y. Sakurada, J. Uozumi, and T. Asakura, "Fresnel diffraction by 1-D regular fractals," Pure Appl. Opt. **1**, 29–40 (1992).
18. M. J. Yzuel and J. Santamaria, "Polychromatic optical image diffraction limited system and influence of the longitudinal chromatic aberration," Opt. Acta **22**, 673–690 (1975).